RESEARCH ARTICLE

Development of Piribedil Solid Lipid Nanoparticles Incorporated in Nasal *In-situ* Gel by DoE

Chekkilla Bhargavi[1,2], Pathuri Raghuveer[1*]

[1]*Department of Pharmaceutics, GITAM School of Pharmacy (Deemed to be University), Hyderabad, Telangana, India.*
[2]*Department of Pharmaceutics, Sarojini Naidu Vanita Pharmacy Maha Vidyalaya, Hyderabad, Telangana, India.*

Received: 06th October, 2023; Revised: 24th November, 2023; Accepted: 25th January, 2024; Available Online: 25th March, 2024

ABSTRACT

Solid lipid nanoparticles (SLNs) are a promising drug delivery platform for regulated, controlled release and targeted distribution. The current study aimed to prepare stable piribedil-loaded nanoparticles with optimized intranasal delivery. Using A 3-factor, 3-level Box-Behnken design (BBD), regression analysis, and 3-D response surface methodology (RSM) plots, the influence of independent process variables, like drug-to-lipid ratio, conc of poloxamer 407 and conc of glyceryl monostearate, on dependent variables, such as entrapment effectiveness and the vesicle size of piribedil SLNs, was assessed. The formulated SLNs exhibit a spherical morphology and exhibit a low degree of crystallinity. The nanoformulation exhibited a higher release of medication compared to the piribedil suspension. The 12-hour drug release demonstrated the use of controlled-release medicine delivery. By adding hyaluronic acid to intranasal formulations, the average particle size (PS), polydispersity index (PDI), and zeta potential (ZP) were all considerably raised. The saturation solubility of nanosized piribedil was 7.1 times that of the unprocessed medication. The nanosized formulation had a greater flux than the pure piribedil reference sample. R3 had a permeability coefficient (Kp) of 0.022 cm h^{-1}, while F3 had a higher value of 0.108 cm h^{-1}. Compared to R3, F3 diffused 15.68 µg cm^{-2} of the drug in the first 15 minutes. Because of their large surface area, nanoparticles enhance diffusion. This study reveals that Piribedil-containing SLNs may be more therapeutic than traditional formulations.

Keywords: Piribedil, Intranasal delivery, Box-Behnken design, Solubility, Stability, Diffusion, Solid lipid nanoparticles.

International Journal of Pharmaceutical Quality Assurance (2024); DOI: 10.25258/ijpqa.15.1.31

How to cite this article: Bhargavi C, Raghuveer P. Development of Piribedil Solid Lipid Nanoparticles Incorporated in Nasal *In-situ* Gel by DoE. International Journal of Pharmaceutical Quality Assurance. 2024;15(1):199-209.

Source of support: Nil.

Conflict of interest: None

INTRODUCTION

Traditional drug delivery techniques struggle to cross the blood-brain barrier (BBB) barrier, resulting in inadequate brain parenchyma medication concentrations. Due to BBB penetration issues, many neurological illness treatments are ineffective.In response to these limitations, researchers have developed novel drug delivery methods. Nanotechnology-based techniques, tailored drug carriers, and alternate administration routes aim to overcome the BBB. These strategies aim to improve BBB drug transport, stability, and central nervous system (CNS)-targeted medication efficacy. Research and development are leading to groundbreaking innovations that could change CNS disorder therapy.[1,2]

CNS problems are difficult to treat, although intranasal medication administration may help. Historically, the BBB's impermeability has hindered neurological treatment. The direct nose-to-brain connection afforded by intranasal administration offers an exceptional chance to bypass the BBB and improve medication delivery.[3] The nasal cavity's highly vascularized mucosa and proximity to the brain make it an excellent medication absorption route. Intranasal medication administration is important for CNS-targeted treatments since it speeds up action and may increase bioavailability. Neurodegenerative and psychiatric CNS illnesses require precise and targeted medication delivery to reach brain therapeutic concentrations.[4] The unique intranasal medication delivery method meets the complex needs of CNS illnesses, optimizing therapeutic success while minimizing systemic effects. This dynamic paradigm shift could revolutionize neurotherapeutics and CNS-related precision medicine.[5]

The dopamine agonist piribedil treats Parkinson's disease and restless legs syndrome. Oral piribedil activates dopamine receptors, notably D2 and D3 receptors, agonistically and antagonistically. It relieves motor symptoms in Parkinson's disease by compensating for dopamine deficiency. Piribedil also reduces leg movement *via* altering dopamine receptors. Gastrointestinal issues, dizziness, and drowsiness require close management. People with cardiovascular difficulties should be

**Author for Correspondence: rpathuri@gitam.edu*

cautious owing to blood pressure and heart rate consequences.[6] Piribedil, a 50-mg pill, has been used clinically since 1969. Piribedil has been used in clinical practice for years but has faced many obstacles.[7] Its oral bioavailability is less than 10%, limiting its efficacy. Piribedil's short biological half-life means it stays in the body at a therapeutic concentration for a short time. To improve piribedil's clinical efficacy and therapeutic potential, additional formulations or modes of administration must be explored.[8]

SLNs are a promising medication delivery vehicle for controlled release and targeted distribution.[9] SLNs use high-pressure homogenization and solvent emulsification-evaporation to control PS and distribution.[10] They are made of solid lipids at physiological temperatures. SLNs are stable due to their biocompatible lipid contents, making them an attractive colloidal solution for medication solubility, bioavailability, and controlled release. SLNs are used in gene therapy, targeted medication delivery, and poorly soluble drug delivery. This introduction shows how SLNs can overcome drug delivery system restrictions and advance pharmaceutical and scientific research.[11] An effective medication delivery system requires optimizing SLN composition. An adequate lipid matrix, a surfactant for stabilization, drug-lipid compatibility for effective encapsulation, PS distribution management, and high drug loading while assuring stability are important.

Pharmaceutical researchers use response surface methodology (RSM), a strong statistical and mathematical tool. RSM lets researchers study complex variable interactions and their effects on desired responses.[12] This strategy streamlines formulation development and helps identify essential SLN parameters, making drug delivery system optimization more reasonable and robust.[13] Box-Behnken design (BBD) statistical experimental design is used in RSM to optimize processes and formulations. This method is excellent for studying how several independent factors affect output while minimizing experimental runs.[14] The BBD helps pharmaceutical researchers study how lipid type, surfactant concentration, and homogenization parameters affect PS, drug loading, and release kinetics in SLNs. This architecture ensures efficient and cost-effective experimental results, optimizing complex pharmaceutical and nanotechnology processes.[15]

MATERIALS AND METHODS

Materials

Enomark Healthcare Pvt. Ltd., Dhamatwan, Gujarat, India, generously gifted piribedil. Sigma Aldrich supplied Trimyristin, tripalmitin, tristearin, sodium taurocholate, soya lecithin, glyceryl monostearate, and dialysis tubing (MW cut-off 12-14 kDa). Tween®80 from SD Fine Chem Ltd (Mumbai, India) and Poloxamer-407 and PVA from Dr. Reddy's Laboratories Ltd., India, were essential ingredients. Analytical-grade chemicals and solvents from the investigation could be utilized unpurified.

Methods

Optimization of critical parameters using design of experiments

Pharmaceutical product design should focus on patient needs and performance. A complete pharmaceutical development strategy includes defining the quality target product profile, identifying CQAs, selecting a manufacturing process, establishing a control strategy, and recognizing material attributes and development parameters that influence CQAs. A systematic methodology simplifies product development and lifetime innovation. This work minimised PS and maximised SLN drug encapsulation using a factorial approach. Piribedil SLN formulation optimization took two steps. The dependent and independent variables were identified *via* exploratory experiments. The optimal parameters were then established using BBD.[16]

The usual parametric design of experiments (DoE) is resource-intensive, time-consuming, and hard to capture factor interactions. This method is inefficient in determining optimal circumstances and factor interactions. Statistical experimental design is more reliable for examining factor impacts on characterization properties and discovering optimal conditions with few runs. This study used the BBD with three variables at three levels to determine how parameters affect PS and encapsulation efficiency (EE). This method improves on one-factor-at-a-time research and screening trials by revealing factor interactions and their effects on pharmaceutical formulation properties.[17]

DoEs

Piribedil-loaded SLN formulation factors were optimized using BBD. Initial tests showed that the drug-to-lipid ratio (A), Poloxamer 407 concentration (B), and glyceryl monostearate concentration (C) significantly affected SLN PS (Y1) and EE (Y2). According to preliminary studies, Table 1 indicates each independent variable's range. Stat-Ease Design Expert® V13.0.5.0's BBD model randomly arranged 17 model experiments. All investigations employed continual homogenization (8000 rpm), sonication (10 minutes), stirring (1000 rpm), and time (3 hours). Table 2 contains all model experiment settings. Following planned experiments, Table 2 illustrates the dependent variables, PS (Y1) and EE (Y2).

Response Measurement

PS and EE

A Malvern PS analyzer using dynamic light scattering (DLS) measured the prepared preparation's average PS. All tests were done in triplicate and diluted with Milli Q water before measurement for accuracy. To test EE, a 10-milliliter SLN solution was spun at 10,000 revolutions per minute for 20 minutes at room temperature. A Shimadzu 1800 spectrophotometer was used to assess the drug's absorbance in the supernatant at λ_{max} 239.2 nm after the lipid component had been isolated. For a reliable drug encapsulation assessment in SLNs, the following equation determined the percentage of EE.[18]

$$EE\ (\%) = \frac{\text{Total drug (mg)} - \text{Free drug (mg)}}{\text{Total drug (mg)}} \text{ X } 100$$

Analysis of Data

Models like linear, quadratic, and cubic explained the complicated interaction between dependent and independent factors. The model's *p-value*, lack of fit, multiple regression coefficients (R2), modified R2, and coefficient of variation were examined to select a suitable model. For model selection, words with *p-values* larger than 0.0005 were considered unimportant and excluded. Equation[19] shows how a quadratic model with multiple regression analysis evaluated each response parameter.

Table 1: List of dependent and independent variables in BBD

Independent variables			*Levels*		
Variable	*Name*	*Units*	*-1*	*0*	*+1*
A	Drug-to-lipid ratio	-	0.1	0.3	0.5
B	Conc. of poloxamer 407	mg	5	7.5	10
C	Conc. of glyceryl monostearate	mg	2	4	6
Dependent variable			Goal		
Y1	PS	Nm	Minimize		
Y2	EE	%	Maximize		

$$Y = A_0 + A_1 X_1 + A_2 X_2 + A_3 X_3 + A_{11} X_1^2 + A_{22} X_2^2 + A_{33} X_3^2 + A_{12} X_1 X_2 + A_{13} X_1 X_3 + A_{23} X_2 X_3$$

Where,

Y	–	Response parameter
A_0	–	Intercept
A_1, A_2, A_3	–	linear regression coefficients
A_{11}, A_{22}, A_{33}	–	quadratic regression coefficients
A_{12}, A_{23}, A_{13}	–	interaction regression coefficients
X_1, X_2 and X_3	–	Main influencing factors
X_1X_2	–	Interactive effect
X_1^2, X_2^2& X_3^2	–	Quadratic effect

Preparation of Piribedil-loaded SLNs

SLNs were formulated using a single emulsification process and solvent evaporation.[20] Piribedil (100 mg), trimyristin (Dynasan-114), and glyceryl monostearate were dissolved in 3 mL chloroform and added to 10 mL 1.5% w/v poloxamer 407. The dispersion was sonicated for 10 minutes after 8 minutes of homogenization at 8000 rpm. The mixture was stirred for 3 hours at 1000 rpm. Nanoparticles were centrifuged at 12000 rpm for 45 minutes and washed with MilliQ water 3 to 4 times. The next stage was lyophilization using trehalose dihydrate as a cryoprotectant to preserve nanoparticle integrity.

Characterization of SLNs

Quantification of PS, PDI, and ZP of SLN

Zetasizer assessed SLN size, PDI, and ZP. In order to get 50 to 200 Kcps for measurements, the obtained SLN dispersion was diluted to 5 mL using double distilled water.

Table 2: BBD with perceived responses

Run	*Drug to lipid ratio (A)*	*Conc. of poloxamer 407 (B)*	*Conc. of glyceryl monostearate (C)*	*PS(Y1)*	*EE(Y2)*
1	0.3	7.5	4	72.18	82.63
2	0.3	7.5	4	69.34	81.34
3	0.3	5	2	124.12	75.12
4	0.3	10	2	67.32	85.43
5	0.1	7.5	2	64.78	88.56
6	0.5	7.5	6	91.64	95.76
7	0.1	7.5	6	37.14	93.42
8	0.5	5	4	145.38	86.12
9	0.3	7.5	4	67.88	81.18
10	0.5	10	4	98.73	93.78
11	0.3	10	6	53.34	88.24
12	0.3	7.5	4	71.76	83.35
13	0.5	7.5	2	114.32	95.32
14	0.1	5	4	93.58	78.75
15	0.1	10	4	50.12	92.82
16	0.3	5	6	87.12	78.76
17	0.3	7.5	4	73.42	80.73

Determination of EE and drug loading

SLNs dispersion (10 mL) was centrifuged at 10,000 rpm in a tube at room temperature for 20 minutes. The lipid fraction was separated and drug absorbance was evaluated at λ_{max} 239.2 nm. The following formulas evaluated drug loading and EE.[21]

$$DL\ (\%) = \frac{Loaded\ drug\ (mg)}{Total\ lipid\ in\ the\ formulation\ (mg)}\ X\ 100$$

$$EE\ (\%) = \frac{Total\ drug\ (mg) - Free\ drug\ (mg)}{Total\ drug\ (mg)}\ X\ 100$$

Morphology by transmission electron microscopy

Transmission electron microscopy (TEM) examined nanoparticle morphology. After being freeze-dried, the piribedil SLNs were diluted with 100% distilled water. The sample holder was placed with a drop and left to air-dry. Imaging occurred, various magnifications were used to observe the sample at 15000 volts in a high vacuum.

Characterization of crystallinity by powder X-ray diffractometry

Powder X-ray diffractometry (PXRD) was performed using nickel-filtered CuKa radiation (40 kV, 30 mA) with a 2° to 70° scan, 0.045° step size, and 0.5 seconds step time. Pure piribedil, a 1:1 drug-lipid combination, and drug-loaded lyophilized SLNs were PXRD samples.

Drug content

To find the drug concentration of the SLN formulations, 10 mg of the sample was dissolved in 50 mL of 0.1 N HCl. The solution was filtered and examined following 24 hours of stirring at room temperature using a magnetic stirring bar set at 400 rpm. The UV spectrophotometer measured the concentration at 239.2 nm.

Dissolution study and release kinetics

The modified paddle method was utilized to know the dissolve rates of piribedil, physical mixture, and SLN formulation. About 5 mg of pure piribedil or SLN formulation in 100 mL PBS, pH 7.4 was utilized. The paddles rotated 100 rpm at 37°C. At 5, 10, 15, 30, 60, 90, and 120 minutes, 5 mL aliquots were filtered. Piribedilconcs were determined at 239.2 nm using UV-visible spectroscopy. Removed aliquots were replenished. Add 0.1% Tween 80 to the dissolving media to maintain sink.[22] To find out how the medication was released, researchers fitted the outcomes from the *in-vitro* release studies to kinetic models such as zero-order, first-order, Higuchi's, and Korsemeyer Peppa's. Piribedil release from SLN formulation was calculated using curve fitting. Several kinetic models fit *in-vitro* release data.[23,24]

Stability studies

The stability of SLN preparation was tested by diluting one milliliter of nanoformulation (≈ 10 mg piribedil) with milli-Q water in three folds (10, 50, and 100 folds). A PS analyzer (Horiba Scientific, USA) assessed each sample's PS using dynamic light scattering (DLS). In three storage conditions (4, 25, and 35°C), SLN formulation thermal stability was examined. Different time points showed SLN formulation morphological alterations. The powdered and diluted SLN formulations were preserved at 4°C, room temperature, and 40°C/75% RH to test their storage stability. Critical characteristics, including PS and ZP were examined at various times.

In-situ gel preparation

The *in-situ* gel formulations were made by combining lyophilized SLN powder with hyaluronic acid. These formulations were diluted with 0.2% w/v egg lecithin to attain the appropriate concentrations. The formulations were refrigerated at 4°C for 24 hours to complete polymer dissolution. Reference samples were parallel samples we developed as a reference. The nasal formulations and reference samples contain piribedil and hyaluronic acid at 10 & 2 mg/mL, 10 & 5 mg/mL, and 10 & 10 mg/mL. The nasal formulations and reference samples included the same piribedil and hyaluronic acid concentrations in 0.2% egg lecithin. Note that the reference samples' piribedil was added unprocessed. However, ULTRA-TURRAX® homogenizers (GmbH, Germany) homogenized raw piribedil powder with hyaluronic acid and 0.2% w/v egg lecithin to create reference samples. Homogenization took 10 minutes at 5000 rpm.[25,26]

In-situ gel formulation - Characterisation and evaluation

The pH of the intranasal preparations was determined using a digital pH meter after diluting them with distilled water. The intranasal formulations were viscosity tested using a Brookfield Rotational Viscometer (DV2T) with a C 16-1 spindle at 10 rpm.[27] A precise amount of the formulation (10 mg) was dissolved in 50 mL of 0.1 N HCl to determine drug content. After 24 hours of stirring at room temperature with a magnetic stirrer at 400 rpm, the solution was filtered and analyzed at 239.2 nm with a UV spectrophotometer. Intranasal formulation PS were measured with a PS analyzer. Dilution with milli-Q water reduced light scattering. The same equipment measured ZP with an electrode on polystyrene electrophoretic cells. Triplicate measurements were taken.

In-vitro drug release study - In-situ gel formulation

In-vitro drug release from the *in-situ* gel preparation was assessed using an artificial nasal fluid medium with precise NaCl, KCl, and CaCl2 concentrations at pH 5.6. The trial began with 200 mg of the intranasal formulation and its reference in a dialysis bag. These bags were dialyzed against 100 mL of dissolving media in a dialysis chamber. The temperature was kept at 37 ± 0.5°C and the paddle speed was kept at 100 rpm. Predetermined intervals of 5 mL dissolving medium samples were taken throughout the experiment. Each withdrawal was followed by an equivalent volume of fresh dissolving medium to maintain experimental conditions. To ensure accurate analysis, materials were strained through a 0.45-µm filter and analyzed at 239.2 nm using a UV spectrophotometer.[28,29]

Permeability study (In-vitro)

A vertical Franz diffusion cell with custom-sized synthetic polyvinylidene fluoride membranes was used for permeability

studies. Pre-saturating the membrane with isopropyl myristate improved drug penetration. We applied 200 mg of intranasal formulation to the membrane in the donor phase.[30,31] Construction of the vertical Franz diffusion cell system was meticulous. In the donor compartment, the intranasal formulation-loaded membrane was placed. Preheated PBS at pH 7.4 was kept in the acceptor compartment at 37°C. A 300-rpm magnetic stir bar in the acceptor chamber stirred. The diffusion investigation started and progressed at set times. An autosampler took 0.8 mL samples from the acceptor phase at each interval, and fresh phosphate buffer was supplied to retain sink conditions. The samples were analyzed with a UV spectrophotometer at 239.2 nm to measure Piribedil diffusion. In equation 2, the drug's flow (J) was estimated by dividing piribedil's permeation through the membrane by the membrane insert's surface area and the experiment's time. Equation 3 used the flux value (J) and donor phase drug concentration to calculate the permeability coefficient (Kp).

$$J = \frac{m}{A.t} \quad (2)$$

where "m" represents the diffused quantity of piribedil, "A" signifies the membrane insert's surface area, and "t" denotes the experiment's duration.

$$JK_p = \frac{J}{Cd} \quad (3)$$

Where "Cd" stands for the initial conc of the drug in the donor phase C.

RESULTS AND DISCUSSION

SLNs have many benefits over conventional colloidal drug delivery technologies, which have drawn attention in recent years. Nanoparticles can be delivered orally, parenterally, dermally, nasally, ocularly, and pulmonaryly, extending their utility. This study used exploratory trials to carefully choose excipients and components that potentially affect crucial quality features. This extensive study attempts to optimize solid lipid nanoparticle formation and medication delivery.

Optimization of Process Variables

Optimizing process variables was key to improving formulation performance. The results showed that increasing homogenization duration and/or speed reduced PS and PDI. Higher speeds apply more force on droplets, resulting in smaller particles. However, increasing homogenization time significantly increased PDI, possibly due to foam production and formulation aggregation. Stirring at 8,000 rpm for 6 min yielded the best results. Following investigations, homogenization/stirring was done at 8,000 rpm for 6 minutes. The coarse emulsion was then sonicated for 5 to 20 minutes to create a nano-emulsion. The finished mixture was agitated to vanish the organic solvent, generating nanoparticles. This stirring method used 500, 1000, and 1500 rpm for optimal optimization for 1, 2, and 4 hours.

DoE reduces process variance and produces nanoparticles with reduced PS and maximum EE. BBD optimized and assessed formulation variables' primary, interaction, and quadratic impacts on PS and EE. BBD is good for quadratic response surfaces and second-order polynomial models. Curvature is estimated using an embedded or fractional factorial design with center and star points. If the distance between the design space center and a factorial point is ±1 unit for each factor, the star point distance is $|\alpha| > 1$. The value of α depends on design aspects and element count. The selected model has substantial PS and PDI values of less than 0.05.

The RSM approach using the BBD required 17 tests. Table 2 shows that factor combinations elicited various responses according to the experimental design. Because they vary greatly overall 17 batches, these results show that the dependent variables are heavily dependent on the independent factors. Stat-Ease Design Expert ® V13.5.0.1 was used to calculate ANOVA, regression coefficients, and regression equations. The experimental results reveal how formulation variables affect solid lipid nanoparticle (SLN) PS and EE. Notably, the systematic change of drug-to-lipid ratio (A), poloxamer 407 (B), and glyceryl monostearate (C) shows their separate and interaction effects. Trends like the negative connection between poloxamer 407 concentration and PS reveal optimization opportunities. However, the dataset shows variability, probably caused by complex formulation component interactions. Replicating conditions and running several experiments may confirm trends and strengthen conclusions.

The factors' multiple linear regression correlations are shown in Table 3. These equations quantify the effects of drug-to-lipid ratio (A), poloxamer 407 (B), glyceryl monostearate (C), and their interaction on PS (Y1) and EE (Y2). A, B, and C coefficients affect Y1 and Y2. Quadratic coefficients and interaction terms have multiple-factor and higher-order terms. Positive signals indicate synergy, whereas negative signs are antagonistic. We fitted data to the quadratic model using backward elimination. Both polynomial equations were significant ($p < 0.01$), as confirmed by ANOVA (Tables 4 & 5) using Design Expert software. Figure 1 indicates a promising correlation between planned and actual results. Experimental and anticipated values for both responses are related. Both models discovered the piribedil SLN process and formulation variables.

Table 2 shows nanoparticle sizes of 37.14 to 145.38 nm. The full comparison showed that the observed values matched the expected values. The PS (Y1) mathematical model had an F-value of 516.16, showing its relevance. Model outputs are very trustworthy, with a 0.01% chance of noise-related

Table 3: Regression equations for the responses – PS& EE

Response	*Regression equation*
Y1	70.92 +25.56A -22.59B -12.66C + 5.76 BC +10.02 A^2 + 16.02 B^2 –3.96 C^2
Y2	81.85 + 2.18A + 5.19B + 1.47 C – 1.60 AB – 1.10 AC + 8.70 A^2 -2.68 B^2 – 2.72 C^2

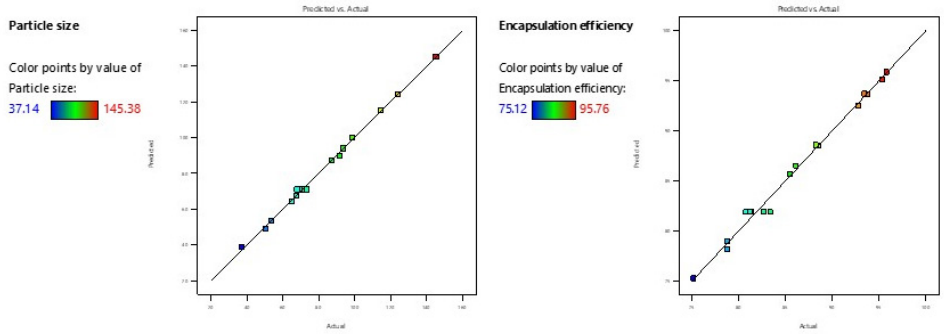

Figure 1: Comparison between predicted and actual values of PS and EE

"Model F-value" ($p < 0.0001$) and a large R2 value of 0.9975. Significant impacts on PS were seen for independent variables A, B, and C, and quadratic terms BC, A2, B2, and C2 ($p \leq 0.0500$). At 0.41, the "Lack of Fit F-value" was not statistically significant relative to pure error, indicating a well-fitting model. The non-significant "Lack of Fit F-value" supports the model's suitability since noise has an 82.20% chance of causing it. The equation showed that A had a greater impact than B and C. Perturbation and 3D RSM plots revealed independent variables' primary and interactive impacts on PS. The perturbation plot (Figure 2) illustrates A, B, and C's main effects on PS (Y1). A has the greatest impact on Y1, followed by B & C, which has a moderate impact. By utilizing 3D RSM and contour plots, the correlation between the dependent and independent variables was elucidated. Figure 2 depicts how B and C interact with PS (Y1) at fixed A. The shapes of RSM plots show how elements interact.

Analysis of residuals and influential points reveals model performance. The residuals—the disparities between actual and anticipated values—show the model's accuracy. Variable residuals indicate the model's capacity to capture observable data. run 7 and Run 17 have larger leverage values, which may affect the model. Internally and externally, studentized residuals assess each data point's influence and deviation significance. Runs 7 and 17 have significant Cook's distance and DFFITS values, impacting the model's fitted values. Standardized order ranks data points by influence. This detailed analysis evaluates the model's robustness and identifies key data points for additional study or refinement.

Table 2 shows that nanoparticle EE ranged from 75.12 to 95.76%. The model is robust because observed and anticipated values correspond closely. The polynomial equation governing EE's 0.9915 correlation coefficient enhances the model's reliability. With an infinitesimal 0.01% likelihood that the Model F-value of 116.56 may be noise, the model is significant. Model terms like A, B, C, AB, AC, A^2, B^2, and C^2 showed significance with "Prob> F" values < 0.0500. Non-significant model terms had values beyond 0.0500. A lack of Fit F-value of 0.18 indicates insignificance relative to pure error, with a 93.56% possibility that it may be noise—a good indicator for a well-fitting model. The equation shows that A decreases EE and B and C increase it. B has a greater impact than A and

Table 4: Analysis of variance of the quadratic model for the response PS (Y1)

Source of variation	*Sum of squares (SS)*	*Degrees of freedom (DF)*	*Mean square value (MS)*	*F-value*	*p-value Prob>F*	
Model	12326.63	7	1760.95	516.16	< 0.0001	significant
A-Drug to lipid ratio	5224.98	1	5224.98	1531.52	< 0.0001	
B-Conc of poloxamer 407	4081.11	1	4081.11	1196.23	< 0.0001	
C-Conc of glyceryl monostearate	1282.71	1	1282.71	375.98	< 0.0001	
BC	132.48	1	132.48	38.83	0.0002	
A^2	422.38	1	422.38	123.81	< 0.0001	
B^2	1080.69	1	1080.69	316.77	< 0.0001	
C^2	66.09	1	66.09	19.37	0.0017	
Residual	30.7	9	3.41			
Lack of fit	10.42	5	2.08	0.4112	0.822	not significant
Pure error	20.28	4	5.07			
Cor total	12357.34	16				

Table 5: Analysis of variance of the quadratic model for the response EE

Source of variation	*SS*	*DF*	*MS*	*F-Value*	*p-value* *Prob>F*	
Model	664.85	8	83.11	116.56	< 0.0001	Significant
A-Drug to lipid ratio	37.98	1	37.98	53.26	< 0.0001	
B-Conc of poloxamer 407	215.49	1	215.49	302.24	< 0.0001	
C-Conc of glyceryl monostearate	17.26	1	17.26	24.21	0.0012	
AB	10.27	1	10.27	14.41	0.0053	
AC	4.88	1	4.88	6.85	0.0308	
A^2	318.66	1	318.66	446.94	< 0.0001	
B^2	30.2	1	30.2	42.35	0.0002	
C^2	31.14	1	31.14	43.68	0.0002	
Residual	5.7	8	0.713			
Lack of fit	0.8821	4	0.2205	0.1829	0.9356	not significant
Pure error	4.82	4	1.21			
Cor total	670.55	16				

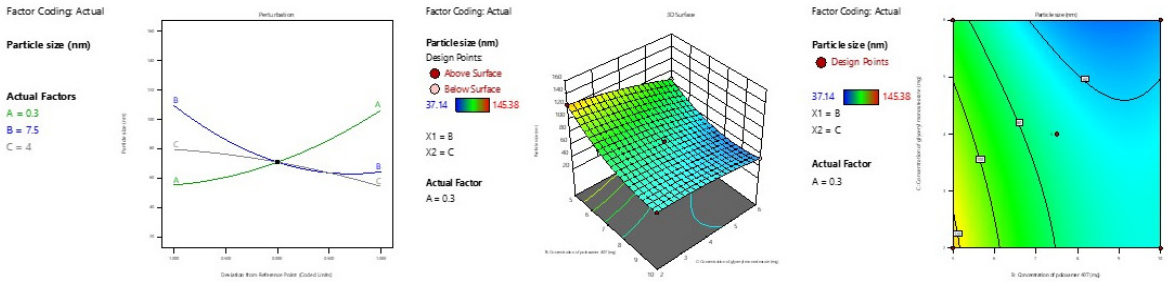

Figure 2: Perturbation, RSM & contor surface plots displaying the effect of A, B, and C on PS

C. The linear effect of A, B, and C on EE is 2.18, 5.19, and 1.47, respectively. AB and AC's negative coefficients indicate antagonistic interactions, indicating their combined effect is less than their individual effects.A positive coefficient for quadratic factors (A^2, B^2, C^2) suggests a curve in the response surface, suggesting non-linear effects of raising or reducing these variables on EE. Perturbation and 3D RSM plots examined how independent variables affected EE. The primary effects of A, B, and C on EE are shown in Figure 3, with linear relationships for Y2. Figure 3 shows the 3D RSM and contour plots for Y2, which reveal factor interactions. It shows the 3D RSM plot of A and B's effect on EE at a fixed C level. 3D RSM plots and contour plots show the interaction between A and C at fixed B levels. These graphs help us understand how variables affect EE.

The residuals, representing the differences between actual and predicted values, indicate how well the model captures the variation in EE. The positive and negative residuals show overestimation and underestimation, respectively, of the EE. Leverage values identify the potential influence of each observation on the model, with higher values suggesting greater impact. Internally and externally, studentized residuals help assess the influence of each data point, and DFFITS quantifies the impact of observations on the fitted values. Cook's distance measures the influence of each point on the entire model, highlighting potential outliers. In this analysis, the model seems generally accurate, with some points exhibiting higher influence and residual values, warranting attention for potential optimization or investigation.

Optimization and Confirmation Experiments

Numerical optimization with desired restrictions determined the best drug-to-lipid ratio (A), poloxamer 407 (B), and glyceryl monostearate (C) concentrations, which affected PS (Y1) and EE(Y2). Figure 4 shows an overlay map of the design space for variables and responses during optimization with a 1.000 desirability score. By identifying process circumstances that produce reliable results, this design-space plot helps build a control strategy. The ideal method conditions were A (0.1), B (9.7), and C (5.9), ensuring a regulated process. Maintaining formulation variables at constant levels ensured thorough SLN formulation preparation. These studies showed exceptional congruence with statistically expected values, demonstrating the optimization process's robustness and accuracy. This match

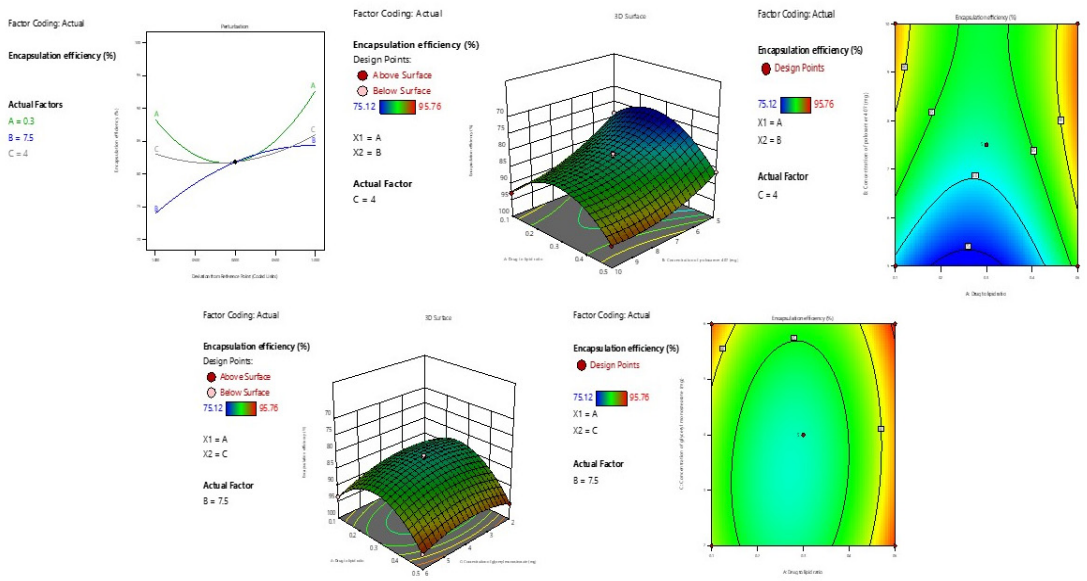

Figure 3: Perturbation, RSM & contor surface plots showing the effect of A, B, and C on %EE

between predicted and observed important technique features confirms the optimization strategy's reliability and precision in providing consistent and desirable SLN formulation results.

Detailed PS distribution and ZP investigation were performed on all formulations. Table 6 shows that the mean size of all formulations ranged from 32.6 ± 5.8 to 34.8 ± 10.1 nm. The PDI range of 0.328 to 0.369 indicated a uniform and homogenous size distribution. Piribedil-enriched SLN formulations had a negative surface charge, indicating its particular orientation within the lipid matrix. The stability of colloidal dispersions relies on surface charge, and the ZP values for SLN formulations ranged from -21.1 ± 1.04 to -23.6 ± 1.06 mV. These ZP values, which vary from -20 to -60 mV, demonstrate the formulations' stability and suitability for colloidal systems. Short-term stability values around 20 mV indicated good stability for piribedil nanoparticles. The formulation's success depends on its stability. Additionally, nanoparticle charge affects intestine absorption dynamics. The negative surface charge of these nanoparticles may promote intestinal permeability through Peyer's patches and lymphatic absorption. In contrast, nanoparticles having a negative surface charge repel each other in the gastrointestinal mucus layer, preventing entanglement. The produced nanoparticles' intestinal permeability may increase. Under careful analysis, the total encapsulation effectiveness of nanoparticle formulations ranged from 95.35 ± 1.92% to 97.58 ± 1.14%.

TEM Analysis

TEM showed spherical particles. Images in Figure 5 confirmed nanoparticle size. DLS particle size measurements matched TEM results.

XRD

Figure 6 shows piribedil and nanoformulation XRD patterns. Piribedil's XRD shows typical crystalline peaks, but the formulation has lost them. The removal of drug peaks indicates amorphization .

After determining the drug content, the sample quantities were carefully selected to ensure that the measured drug content was within 97.82 to 99.34% of the theoretical drug content. Figure 7 displays the *in-vitro* piribedil release curve from SLN in PBS, pH 7.4. The nanoformulation released more medicine than the piribedil suspension. Piribedil is hydrophobic therefore its solubility rises in nanoparticles, resulting in a faster and better release. Controlled-release medication delivery was evident in the 12-hour drug release.

Optimized formulation drug release data was tailored into kinetic equations to know the drug release sequence and mechanism. The release profile followed first-order kinetics (R2 = 0.99405).

The regression coefficient value is closer to unity in firstorder kinetics, indicating that concentration change is the only factor affecting time change (Table 7).

Stability Studies

Piribedil nanocrystals were tested for stability at 4 ± 2, 25 ± 2, and 37 ± 2 °C for six months to see how storage conditions affect performance. Mean PS, PDI, and ZP values at various intervals are shown in Table 8. Piribedil SLN formulation was stable during the six-month investigation. At 3 and 6 months, PS and PDI changed significantly, especially at higher temperatures, emphasizing the need for exact storage conditions for SLN formulation features. However, ZP values remained within an acceptable range, demonstrating surface charge stability under measured conditions.

Hyaluronic acid-derived SLN intranasal administration devices were viscous. Each of the three formulations exceeded 95% drug content. The formulations' pH values were 5.5 to 6.5, as recommended for nasal administration (nasal mucosa pH: 4.5–6.5). The mean PS, PDI, and ZP of intranasal formulations

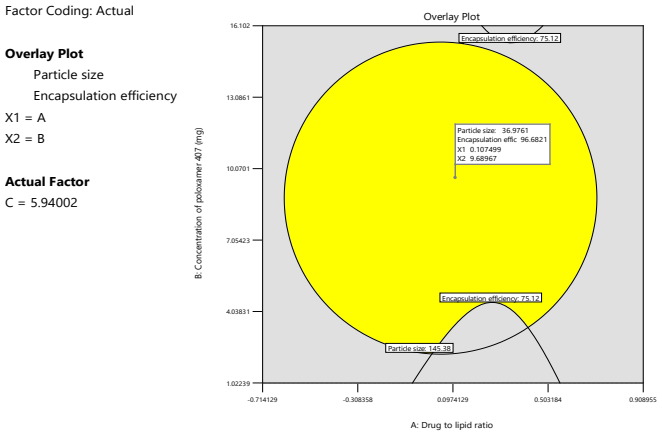

Figure 4: Overlay plot showing the design space

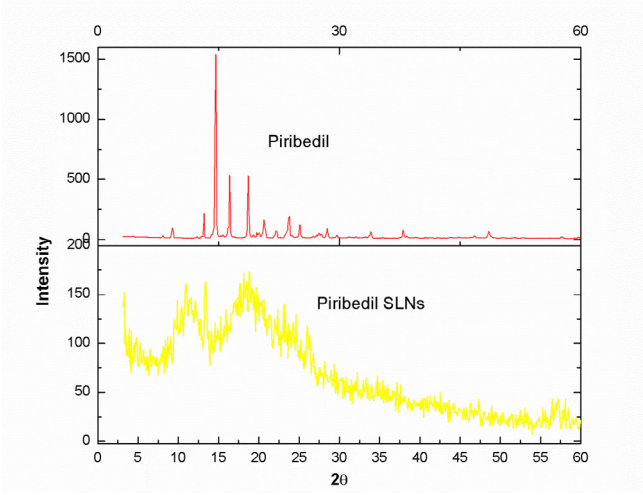

Figure 6: XRD pattern of piribedil SLNs

Table 6: The mean PS, PDI, ZP, and EE of optimized formulations

Batch	*MPS ± SD (nm)*	*PDI*	*ZP ± SD (mV)*	*%EE ± SD*
F1	33.8 ± 3.1	0.347	-21.1± 1.04	95.35 ± 1.92
F2	32.6 ± 2.8	0.328	-22.5 ± 2.17	96.12 ± 1.36
F3	34.8 ± 1.1	0.369	-23.6 ± 1.06	97.58 ± 1.14

n = 3 ($p < 0.05$)

increased significantly with hyaluronic acid. PS increases due to hyaluronic acid coating. Hyaluronic acid increased the formulation's negative charge. Table 9 shows how hyaluronic acid affects intranasal formulations' mean PS, PDI, and ZP.

In water, piribedil is poorly soluble. Intranasal dissolution was compared to pure piribedil reference formulations. Piribedil dissolving from different formulations during 5 to 120 minutes is seen here. The values are the mean ± SD of three replicates (n = 3). Dissolution rates vary between F1-F3 and R1-R3, demonstrating that formulation composition affects drug release kinetics. Different formulations have lower solubility than F3. In the first 15 minutes, 15.48 ± 0.94% of the medication was released from F3, compared to 3.27 ± 0.64% from R3. Nanosizing processes may explain these dissolution rate differences, as tiny particles have a higher surface area than microparticles. The Noyes-Whitney equation predicts disintegration. Piribedil nanosizing exhibited 7.1-fold saturation solubility over the raw drug. Figure 8 shows intranasal formulation dissolution profiles.

Piribedil was tested for diffusion through a 100-nm synthetic membrane. Due to their pore size, piribedil nanoparticles might penetrate through the membrane. Nanoparticle surface area was critical to passive diffusion. Due to increased drug solubility, intranasal formulations diffused faster than reference samples (Figure 9). Piribedil diffused immediately from the intranasal formulation (F3) but took 10 minutes from the reference formulation (R3). F3 had a substantially higher flux (J) of piribedil permeating 1 cm^2 of the membrane within 1 hour compared to R3 (32.43 ± 1.14 vs. 6.06 ± 0.48 µg cm^{-2} h^{-1}). Piribedil nanoparticles, especially those containing Hyaluronic acid, helped penetrate the synthetic membrane. The nanosized formulation had a flux higher than the pure Piribedil reference sample. The permeability coefficient (Kp) of F3 was larger than R3, with values of 0.108 and 0.022 cm h^{-1}, respectively. In the first 15 minutes, 15.68 µg cm^{-2} of the drug diffused from F3 compared to 0.73 µg cm^{-2} from R3. Nanoparticles boost diffusion due to their surface area.

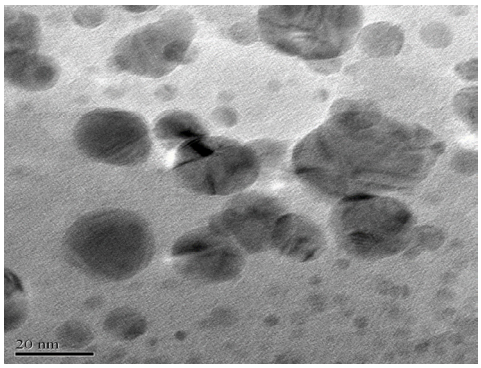

Figure 5: TEM image of piribedil SLN

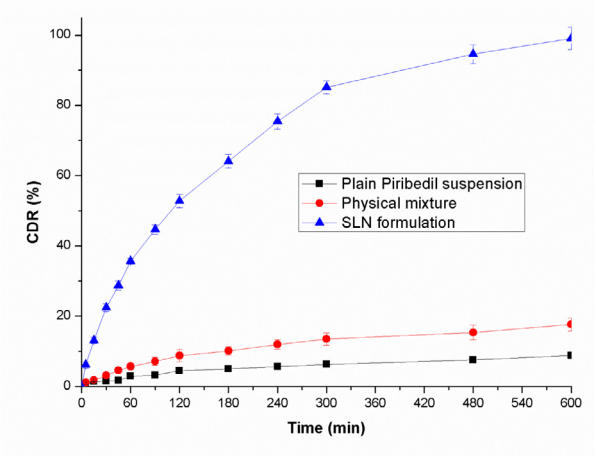

Figure 7: *In-vitro* drug release pattern of piribedil

Table 7: Release kinetics of optimized formulation of piribedil SLNs

Formulation Code	*Zero Order*		*First Order*		*Higuchi*		*Korsemeyer-Peppas*	
	R^2	*n*	R^2	*n*	R^2	*n*	R^2	*n*
F1	0.8988	4.2292	0.99405	-0.0523	0.98013	22.2266	0.9779	65.4084

Table 8: Results of stability studies

Duration (Month)	*Stored at 4 ± 2°C*			*Stored at 25 ± 2°C*			*Stored at 37 ± 2°C*		
	PS (nm)	*PDI*	*ZP (mV)*	*PS (nm)*	*PDI*	*ZP (mV)*	*PS (nm)*	*PDI*	*ZP (mV)*
0	33.8 ± 3.1	0.347 ± 0.005	-21.1 ± 1.04	34.78 ± 2.14	0.328 ± 0.005	-22.6 ± 1.76	36.78 ± 2.27	0.318 ± 0.005	-22.5 ± 1.54
3	34.12 ± 3.32	0.332 ± 0.005	-22.7 ± 0.87	37.92 ± 1.86	0.346 ± 0.005	-23.1 ± 1.28	58.88 ± 1.87	0.423± 0.005	-23.12 ± 2.12
6	34.59 ± 3.46	0.348 ± 0.005	-21.8 ± 1.21	40.92 ± 1.67	0.388 ± 0.005	-24.2 ± 1.32	78.34 ± 3.58	0.532 ± 0.005	-21.32 ± 1.76

n = 3

Table 9: The average PS, PDI, and ZP values of intranasal formulations

Batch	*Average PS (nm)*	*PDI*	*ZP*
F1	46.0 ± 1.12	0.327 ± 0.005	- 17.92 ±1.13
F2	44.6 ± 3.21	0.317 ± 0.005	- 20.7 ± 1.32
F3	49.8 ± 2.13	0.284 ± 0.005	- 16.9 ± 2.21

n = 3

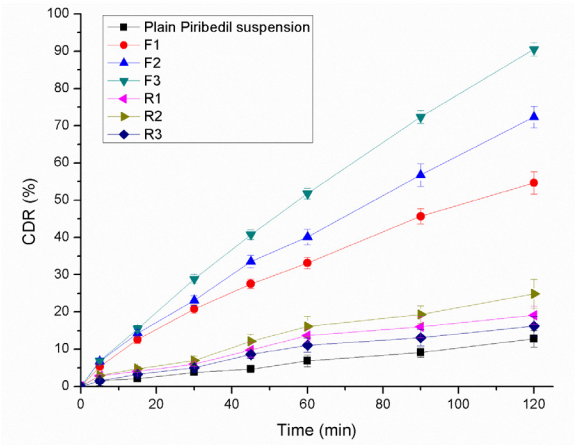

Figure 8: Dissolution pattern of piribedil intranasal formulations

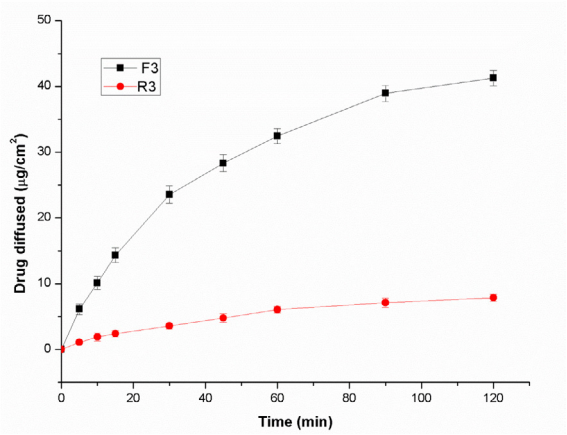

Figure 9: *In-vitro* permeability of intranasal formulations

CONCLUSION

The work created stable piribedil-loaded nanoparticles with optimized intranasal delivery. The formulations improved drug content, solubility, and penetration. Stability over six months at varied temperatures enables long-term storage. These nanoparticles may improve clinical outcomes in piribedil delivery, particularly intranasal dosing. *In-vivo* and clinical trials are needed to confirm these encouraging results and evaluate this nanotechnology-based medication delivery strategy. This study optimized piribedil nanoparticle formulation factors using a 3-factor, 3-level BBD, regression analysis, and 3-D RSM plots. The prepared SLNs have a spherical shape and poor crystalline structure. Piribedil nanoformulation increased dissolution. This study reveals that piribedil-containing solid lipid nanoparticles may be more therapeutic than traditional formulations.

ACKNOWLEDGEMENTS

To conduct this research, the writers are grateful to the administration of GITAM University in Hyderabad, Telangana, India, for making the necessary facilities available. The student would also want to thank management and faculty of Sarojini Naidu Vanita Pharmacy Maha Vidyalaya, Hyderabad, Telangana, India for all the help and encouragement they've given them.

REFERENCES

1. Mittal KR, Pharasi N, Sarna B, Singh M, Rachana, Haider S, Singh SK, Dua K, Jha SK, Dey A, Ojha S. Nanotechnology-based drug delivery for the treatment of CNS disorders. Translational Neuroscience 2022;13(1):527-546.
2. Nayab DE, Din FU, Ali H, Kausar WA, Urooj S, Zafar M, Khan I, Shabbir K, Khan GM. Nano biomaterials based strategies for enhanced brain targeting in the treatment of neurodegenerative diseases: an up-to-date perspective. Journal of Nanobiotechnology 2023;21(1):477.
3. Du L, Chen L, Liu F, Wang W, Huang H. Nose-to-brain drug delivery for the treatment of CNS disease: New development and strategies. International Review of Neurobiology 2023;171:255-297.
4. Jeong SH, Jang JH, Lee YB. Drug delivery to the brain via the nasal route of administration: Exploration of key targets and major consideration factors. Journal of Pharmaceutical

Investigation 2023;53(1):119-152.
5. Keller LA, Merkel O, Popp A. Intranasal drug delivery: Opportunities and toxicologic challenges during drug development. Drug Delivery and Translational Research 2021:1-23.
6. Perez-Lloret S, Rascol O. Piribedil for the treatment of motor and non-motor symptoms of Parkinson disease. CNS Drugs 2016;30:703-717.
7. Uppuluri CT, Ravi PR, Dalvi AV. Design, optimization and pharmacokinetic evaluation of piribedil loaded solid lipid nanoparticles dispersed in nasal in situ gelling system for effective management of Parkinson's disease. International Journal of Pharmaceutics 2021;606:120881.
8. Mittur A. Piribedil: Antiparkinsonian properties and potential clinical utility in dopaminergic disorders. Current Drug Therapy 2011;6(1):17-34.
9. Javed S, Mangla B, Almoshari Y, Sultan MH, Ahsan W. Nanostructured lipid carrier system: A compendium of their formulation development approaches, optimization strategies by quality by design, and recent applications in drug delivery. Nanotechnology Reviews 2022;11(1):1744-1777.
10. Viegas C, Patrício AB, Prata JM, Nadhman A, Chintamaneni PK, Fonte P. Solid Lipid Nanoparticles vs. Nanostructured Lipid Carriers: A Comparative Review. Pharmaceutics 2023;15(6):1593.
11. Mishra V, Bansal KK, Verma A, Yadav N, Thakur S, Sudhakar K, Rosenholm JM. Solid lipid nanoparticles: Emerging colloidal nano drug delivery systems. Pharmaceutics 2018;10(4):191.
12. Vakilinezhad MA, Tanha S, Montaseri H, Dinarvand R, Azadi A, Javar HA. Application of response surface method for preparation, optimization, and characterization of nicotinamide loaded solid lipid nanoparticles. Advanced Pharmaceutical Bulletin 2018;8(2):245.
13. Priyanka K, Sahu PL, Singh S. Optimization of processing parameters for the development of Ficusreligiosa L. extract loaded solid lipid nanoparticles using central composite design and evaluation of antidiabetic efficacy. Journal of Drug Delivery Science and Technology 2018;43:94-102.
14. Nekkaa A, Benaissa A, Lalaouna AE, Mutelet F, Canabady-Rochelle L. Optimization of the extraction process of bioactive compounds from Rhamnusalaternus leaves using Box-Behnken experimental design. Journal of Applied Research on Medicinal and Aromatic Plants 2021;25:100345.
15. Ahmad A, Rehman MU, Wali AF, El-Serehy HA, Al-Misned FA, Maodaa SN, Aljawdah HM, Mir TM, Ahmad P. Box–Behnken response surface design of polysaccharide extraction from rhododendron arboreum and the evaluation of its antioxidant potential. Molecules 2020;25(17):3835.
16. Yu LX, Amidon G, Khan MA, Hoag SW, Polli J, Raju GK, Woodcock J. Understanding pharmaceutical quality by design. The AAPS Journal2014;16:771-783.
17. Williamson EM, Sun Z, Mora-Tamez L, Brutchey RL. Design of Experiments for Nanocrystal Syntheses: A How-To Guide for Proper Implementation. Chemistry of Materials 2022;34(22):9823-9835.
18. Soni K, Rizwanullah MD, Kohli K. Development and optimization of sulforaphane-loaded nanostructured lipid carriers by the Box-Behnken design for improved oral efficacy against cancer: In vitro, ex vivo and in vivo assessments. Artificial cells, nanomedicine, and biotechnology 2018;46(sup1):15-31.
19. Anandam S, Selvamuthukumar S. Optimization of microwave-assisted synthesis of cyclodextrinnanosponges using response surface methodology. Journal of Porous Materials 2014;21:1015-1023.
20. Pooja D, Kulhari H, Tunki L, Chinde S, Kuncha M, Grover P, Rachamalla SS, Sistla R. Nanomedicines for targeted delivery of etoposide to non-small cell lung cancer using transferrin functionalized nanoparticles. RSC Advances 2015;5(61):49122-49131.
21. Koehler JK, Schmager S, Bender V, Steiner D, Massig U. Preparation of Nanosized Pharmaceutical Formulations by Dual Centrifugation. Pharmaceuticals 2023;16(11):1519.
22. Mast MP, Modh H, Knoll J, Fecioru E, Wacker MG. An Update to Dialysis-Based Drug Release Testing—Data Analysis and Validation Using the Pharma Test Dispersion Releaser. Pharmaceutics 2021;13(12):2007.
23. Costa P, Lobo JM. Modeling and comparison of dissolution profiles. European Journal of Pharmaceutical Sciences 2001;13(2):123-133.
24. Dash S, Murthy PN, Nath L, Chowdhury P. Kinetic modeling on drug release from controlled drug delivery systems. ActaPoloniaePharmaceutica 2010;67(3):217-223.
25. Mandal S, Thimmasetty MK, Prabhushankar GL, Geetha MS. Formulation and evaluation of an in situ gel-forming ophthalmic formulation of moxifloxacin hydrochloride. International Journal of Pharmaceutical Investigation 2012;2(2):78.
26. Paradkar MU, Parmar M. Formulation development and evaluation of Natamycinniosomal *in-situ* gel for ophthalmic drug delivery. Journal of Drug Delivery Science and Technology 2017;39:113-122.
27. Thakkar H, Patel A, Chauhan N. Formulation and optimization of mucoadhesive microemulsion containing mirtazapine for intranasal delivery. Chronicles of Young Scientists 2014; 5(1):25.
28. Sherafudeen SP, Vasantha PV. Development and evaluation of in situ nasal gel formulations of loratadine. Research in Pharmaceutical Sciences 2015;10(6):466.
29. Omar MM, Eleraky NE, El Sisi AM, Hasan OA. Development and evaluation of *in-situ* Nasal Gel Formulations of Nanosized Transferosomal Sumatriptan: Design, Optimization, in vitro and in vivo Evaluation [Retraction]. Drug Design, Development and Therapy 2022;16:2291-2292.
30. Ng SF, Rouse J, Sanderson D, Eccleston G. A comparative study of transmembrane diffusion and permeation of ibuprofen across synthetic membranes using Franz diffusion cells. Pharmaceutics 2010;2(2):209-223.
31. Salamanca CH, Barrera-Ocampo A, Lasso JC, Camacho N, Yarce CJ. Franz diffusion cell approach for pre-formulation characterisation of ketoprofen semi-solid dosage forms. Pharmaceutics 2018;10(3):148.